Quantifying subclinical and longitudinal microvascular changes following episcleral plaque brachytherapy (EPB) using spectral-domain OCT angiography.

Preprint · November 2019

DOI: 10.1101/860148

11 authors, including:

Bright Ashimatey
Indiana University Bloomington
9 PUBLICATIONS **34** CITATIONS
SEE PROFILE

Melvin Astrahan
University of Southern California
114 PUBLICATIONS **2,750** CITATIONS
SEE PROFILE

Zhongdi Chu
University of Washington Seattle
57 PUBLICATIONS **732** CITATIONS
SEE PROFILE

Ruikang Wang
University of Washington Seattle
757 PUBLICATIONS **14,339** CITATIONS
SEE PROFILE

Title: Quantifying subclinical and longitudinal microvascular changes following episcleral plaque brachytherapy (EPB) using spectral-domain OCT angiography.

Short Title: Longitudinal Analysis of OCTA in EPB-treated eyes.

Authors: Kyle M. Green, MD,*[1] Brian C. Toy, MD,*[1] Bright S. Ashimatey, OD, Ph.D,[1] Debarshi Mustafi, MD, PhD,[1] Richard L. Jennelle, MD,[2] Melvin A. Astrahan, PhD,[2] Zhongdi Chu, MS,[3] Ruikang K. Wang, PhD,[3,4] Jonathan Kim MD,[1,5] Jesse L. Berry, MD,[1,5] Amir H. Kashani, MD, PhD[1,6]

*contributed equally
[1] USC Roski Eye Institute, Department of Ophthalmology, Keck School of Medicine, University of Southern California, Los Angeles, CA.
[2] Department of Radiation Oncology, University of Southern California Norris Comprehensive Cancer Center, Los Angeles, CA.
[3] Department of Bioengineering, University of Washington, Seattle, Washington.
[4] Department of Ophthalmology, University of Washington, Seattle, Washington.
[5]The Vision Center, Children's Hospital Los Angeles, Keck School of Medicine, Los Angeles CA
[6] USC Ginsberg Institute for Biomedical Therapeutics, University of Southern California, Los Angeles, CA

Meeting Presentation: American Society of Retina Specialists Annual Meeting, Vancouver, British Columbia, July 22, 2018.

Financial Support:
AHK: Research support from Carl Zeiss Meditec and National Institutes of Health (NIH grant no. R01EY030564, 1K08EY027006,); the USC Roski Eye Institute receives unrestricted departmental funding from Research to Prevent Blindness.
RKW: Research support from Carl Zeiss Meditec and National Institutes of Health (NIH grant no. R01EY028753).
JLB: Grants from National Cancer Institute of the National Institute of Health Award Number K08CA232344

Communicating Author: Amir H. Kashani MD PhD
Institute for Biomedical Therapeutics
1450 San Pablo St., 6th Floor
Los Angeles, CA 90033
Email: ahkashan@usc.edu

Abbreviations:

EPB	Episcleral Plaque Brachytherapy
FA	Fluorescein Angiography
FIR	Flow Impairment Region
OCT(A)	Optical Coherence Tomography (Angiography)
RR	Radiation Retinopathy
VDI	Vessel Diameter Index
VSD	Vessel Skeleton Density

Abstract

Background: I-125 episcleral plaque brachytherapy (EPB) is standard-of-care for globe-conserving treatment of medium-sized choroidal melanomas. Radiation retinopathy is a potential consequence of treatment, characterized by deleterious effects on retinal microvasculature. We investigated the application of Optical Coherence Tomography Angiography (OCTA) for detecting and longitudinally monitoring I-125 episcleral plaque brachytherapy induced radiation retinopathy.

Methods: High resolution OCTA of the central 3x3mm macula were obtained from I-25 episcleral plaque brachytherapy treated and untreated fellow eyes of 62 patients. Capillary density (vessel skeleton density, VSD) and caliber (vessel diameter index, VDI) were quantified using previously validated semi-automated algorithms. Nonperfusion was also quantified as flow impairment regions (FIR). Exams from treated and fellow eyes obtained pre-treatment and at 6-month, 1-year, and 2-year intervals were compared using generalized estimating equation linear models. Dosimetry maps were used to evaluate spatial correlation between radiation dose and microvascular metrics.

Results: Mean time from treatment to last follow-up was 10.8 months. Mean±SD and median radiation dose at the fovea were 64.5 ± 76 Gy and 32.0 Gy, respectively. Preoperative logMAR (Snellen) mean visual acuity was 0.26 ± 0.05 (~20/35) and 0.08 ± 0.02 (~20/25) in treated and fellow eyes, respectively. At 6 months, treated eyes had significantly lower VSD (0.147 ± 0.003 vs 0.155 ± 0.002; $p = 0.023$) and higher FIR (1.95 ± 0.176 vs 1.45 ± 0.099; $p = 0.018$) compared to fellow eyes. There was a significant decrease in VSD and a corresponding increase in FIR

even for treated eyes without clinically identifiable retinopathy at 6 months. VDI was significantly higher in treated eyes than in fellow eyes at 2 years (2.93 ± 0.022 vs 2.84 ± 0.016; $p = 0.002$). Microvascular changes were spatially correlated with a radiation gradient of 85-250 Gy across the fovea.

Conclusions: OCTA can be used to quantify and monitor EPB induced radiation, and can detect vascular abnormalities even in the absence of clinically observable retinopathy. OCTA may therefore be useful in investigating treatment interventions that aim to delay EPB-induced radiation retinopathy.

Introduction

The development of radiation retinopathy (RR) following treatment of choroidal melanoma with episcleral plaque brachytherapy (EPB) can have deleterious effects on retinal microvasculature that leads to permanent visual decline. The Collaborative Ocular Melanoma Study (COMS) validated EPB as standard-of-care for globe-conserving treatment of medium-sized choroidal melanomas.(1) Despite the selection of iodine-125 (I-125) and gold shielding to minimize adverse radiation effects, visual morbidity remains high, with only 43% of patients maintaining visual acuity of 20/200 or better 3 years after treatment with standard COMS plaques.(2) Some reports indicate that adverse radiation effects can be partially mitigated through the use of 3D conformal treatment planning software and customized collimated plaques to decrease the radiation dose to critical visual structures (e.g. the fovea).(3, 4) The onset of RR varies greatly, ranging from as early as 1 month to 15 years, but it most commonly occurs between 6 months and 3 years after treatment.(5) The location of the tumor, and thus the dose to the fovea, is critical but not the sole risk factor. RR is primarily a vascular disease and shares many clinical features with diabetic retinopathy including damage to capillaries, which leads to variable degrees of hyperpermeability, retinal ischemia, and neovascularization.(6)

While clinical features of RR, including dot-blot hemorrhages, microaneurysms, and macular edema can be seen on exam, as with diabetic retinopathy, there is underlying damage present before these clinical features manifest. Fluorescein angiography (FA) can reveal early areas of non-perfusion and vascular leakage.(7-9) OCT angiography (OCTA) has been used to non-invasively demonstrate morphologic features of microvasculature with excellent resolution.(10-13) By generating detailed depth-resolved images, OCTA can potentially be used to detect and

monitor capillary-level aberrations in blood flow at multiple timepoints early in the course of RR. To date, there have been a few studies that employ OCTA to assess microvascular changes in RR. Two recent studies used binarized OCT angiograms to demonstrate a decrease in parafoveal (14, 15) and peripapillary capillary (16, 17) density in irradiated eyes compared to fellow eyes. To our knowledge, no studies have performed longitudinal analysis to identify early microvascular changes (prior to 1 year) in treated eyes, nor have any used OCTA to explore a possible spatial correlation between these changes and radiation dose.

In the present study, we employed longitudinal analysis of OCT angiograms to further determine what quantifiable morphologic differences exist in the microvasculature between treated and fellow eyes over time, as well as how early in the course of RR these differences can be detected. More specifically, we used previously described OCTA metrics, (11, 18) vessel skeleton density (VSD) and vessel diameter index (VDI), to quantitatively assess changes in retinal vascular networks. We have previously employed these metrics to quantify vascular density and diameter in diabetic retinopathy and uveitis.(11, 13) We also report flow impairment region (FIR), which is further detailed in the methods section, to quantify areas of subclinical non-perfusion larger than a set threshold.

Methods

Approval for this study was obtained from the Institutional Review Board of the University of Southern California, and the described research adhered to the tenets of the Declaration of Helsinki. This was a retrospective, consecutive series of 62 adult patients treated with I-125 episcleral plaque brachytherapy (EPB) for medium sized choroidal melanoma by one of two

ocular oncologists (JB, JK) at the USC Roski Eye Institute. Any subject with history of intraocular melanoma and plaque brachytherapy was eligible for inclusion. Treatment planning and surgery were performed as previously described with stereotactic plaque brachytherapy radiation treatment planning platform (Plaque Simulator; Eye Physics, LLC; Los Alamitos, CA); a dose of 85 Gy at a rate of 0.5 Gy/hr was prescribed to the apex of the lesion or to 5mm height, whichever was greater with a 2mm margin at the base.(19) Subjects with media opacity impairing visualization of the macula, pre-existing retinal vascular disease (diabetic retinopathy, retinal vein occlusion, choroidal neovascularization), or pre-existing subretinal fluid or macular edema prior to plaque placement were excluded from the study. Subjects with direct tumor involvement in the 3x3mm perifoveal region were also excluded as this was the area assessed by OCTA. Patient demographics, including age and gender, were abstracted from the medical record. Clinical data collected included visual acuity, radiation dose to fovea, follow-up time, and presence of clinically evident radiation retinopathy as determined by the Finger criteria.(8) Visual acuity was reported as logMAR (Snellen equivalent).

OCTA Imaging and Image Analysis

OCTA was performed in both the irradiated eye and the fellow non-irradiated eye for each patient during the patient's regularly scheduled clinic visits. Imaging was performed with a commercially available, FDA-approved, spectral-domain OCTA platform (Angioplex; Zeiss Meditec; Dublin, CA). High resolution 3x3mm OCT angiograms centered on the fovea with a signal strength greater than 7/10 were included for analysis. Images with significant motion artifacts that obscured the vascular architecture were excluded from analysis. For any eye with multiple images on a single date, the highest quality image was chosen. A previously described

semi-automated algorithm was used for quantitative analysis of vessel skeletal density (VSD), vessel diameter index (VDI), and flow impairment region (FIR).(11, 18) Briefly, VSD is defined as a unitless proportion of the total length (in pixels) of all skeletonized vessels divided by the total number of pixels in the image window, which reflects capillary density. VDI is defined as a unitless proportion of the total vessel area divided by the total skeletonized vessel area, which reflects average vessel diameter. Lastly, FIR is defined as the sum of avascular areas in an image larger than a pre-defined threshold area, which in this study was set at $0.002mm^2$ to reflect the maximum threshold for physiologic intercapillary distance. This value was based on an estimate from histologic analysis that the avascular periarteriolar region is ~50μm.(20) A $0.002mm^2$ threshold closely approximates the area of a circle with this diameter.

Data Analyses

The effect of radiation therapy on the OCTA metrics (VSD, FIR and VDI) was assessed longitudinally. Data acquired included pretreatment exams obtained prior to surgery, as well as post-treatment exams binned into 6-month (range 3-9 months), 1-year (range 9-18 months) and 2-year (range 18-30 months) groups. Summary OCTA metrics were compared between irradiated and fellow eyes at the different time intervals using generalized estimating equation (GEE) linear models. In the GEE models, the OCTA metrics were each used as predictor variables of the treatment status of the eyes —irradiated eye versus fellow eye. Summary OCTA metrics for treated eyes were also compared between baseline and the various follow-up timepoints. Statistical significance was defined when the p-value associated with the odds ratio of the univariate model was less than 0.05. GEE models allow for the analysis of longitudinal

repeated measures, as well as correlated fellow eye data.(21) When the number of radiated and fellow eyes were balanced, paired t-statistic or Wilcoxon sign-ranked tests were also used.

The radiation dose-related changes of the OCTA metrics were also investigated. The OCTA metrics between high-dose eyes (foveal radiation >45 Gy) were compared to low-dose eyes (foveal radiation <15 Gy). These thresholds were chosen based on published dose tolerance limits of the retina.(22) A second exploratory approach was adapted to assess if there was spatial correlation between radiation dose and microvascular density within the 3x3mm foveal regions imaged. To evaluate this "within eye" correlation, the last acquired OCT angiograms (over the defined study period) of the irradiated eyes were investigated and five eyes which displayed spatial gradients in microvascular density were subjectively selected for further evaluation. EPB dosimetry maps of these eyes were then generated using Eye Physics Plaque Simulator software (Eye Physics, LLC; Los Alamitos, CA) developed previously at the University of Southern California.(23-25) For each case, dosimetry maps were superimposed on both the original OCT angiograms and their corresponding fundus photos for analysis.

Results

We report the results of 62 participants who underwent EPB therapy. Table 1 summarizes the demographic and clinical characteristics of the study population. Table 2 summarizes the results of the OCTA metrics compared between EPB-treated and untreated fellow eyes.

Table 1. Patient demographics and clinical data.

Total Number of Participants	62
Age, yrs	
Mean±SD	62.9±13.8
Median [IQR]	65.5 [57.0-72.9]
Female Gender (% female)	34 (55.7%)
Follow-up time, yrs	
Mean±SD	0.9±0.4
Median [IQR]	0.9 [0.6-1.3]
Time from plaque to 1st OCTA, yrs	
Mean±SD	1.3±0.8
Median [IQR]	1.3 [0.5-1.9]

Table 2. Clinical and OCTA measures by eye.

Mean±SEM	EPB Treated	Fellow Eye	p-value
Baseline BCVA (LogMAR)	0.26±0.05	0.08±0.02	**<0.001**
Vessel Skeleton Density			
Baseline	0.151±0.003	0.155±0.002	0.256
6 months	0.147±0.003	0.155±0.002	**0.023**
12 months	0.143±0.004	0.156±0.003	**0.013**
24 months	0.142±0.004	0.156±0.002	**0.008**
Vessel Diameter Index			
Baseline	2.85±0.020	2.86±0.012	0.972
6 months	2.85±0.021	2.85±0.016	0.699
12 months	2.91±0.040	2.83±0.013	0.062
24 months	2.93±0.022	2.84± 0.016	**0.002**
Flow Impairment Region			
Baseline	1.65±0.175	1.49±0.120	0.407
6 months	1.95±0.176	1.45±0.099	**0.018**
12 months	2.15±0.230	1.48±0.157	**0.027**
24 months	2.21±0.230	1.45±0.086	**0.007**
Radiation dose, Gy (mean±SD, median [IQR])			
Tumor Apex	99.4±25, 86.8 [85-111]		
Fovea*	64.5±76, 32.0 [18-81]		

*The median dose to the fovea (32 Gy) is below published thresholds for clinically-evident radiation damage (35 Gy). EPB = Episcleral Plaque Brachytherapy.

169 Baseline

170 Prior to EPB, eyes with melanoma had significantly lower visual acuity compared to fellow eyes;
171 however, there were no significant differences in VSD, VDI, or FIR at baseline between eyes
172 with melanoma and the contralateral eyes (Table 2).

173

174 Six Month Follow-Up

175 Fifteen subjects had OCT angiograms at 6 months after EPB. Only one of these (representing
176 6.7%) demonstrated even minimal evidence of radiation retinopathy on clinical examination.
177 However, the VSD and FIR metrics of OCTA assessment showed significantly lower VSD and
178 higher FIR for the treated eyes compared to fellow eyes respectively (Table 2). These changes
179 can also be appreciated qualitatively in maps of VSD and FIR (Figure 1). Importantly, among
180 treated eyes that had no clinically identifiable radiation retinopathy at this follow-up period, and
181 also had pre-treatment exams for direct comparison (n=5), there was still a significantly
182 decreased VSD (0.146±0.011 [6 months] vs 0.158±0.005 [baseline]; $p = 0.035$) and an increased
183 FIR (1.76±0.665 [6 months] vs 1.28±0.339 [baseline]; $p = 0.043$).

184

185 **Fig 1. Processed OCT angiograms from treated and fellow eyes of a single patient.**
186 OCT angiograms from the treated (OS) and fellow eye (OD) of a 20-year-old female
187 demonstrate marked qualitative differences in parafoveal vessel density (column 1). The OCT
188 angiogram of each eye was obtained 263 days (8.6 months) following placement in the treated
189 eye with a 46.0 Gy dose at the fovea. Visual acuity at the time of image acquisition was 20/350
190 in the treated eye and 20/20 in the fellow eye. Skeletonized OCT angiograms with accompanying
191 skeleton density heat maps were generated (columns 2 and 3). Warmer colors reflect areas of
192 greater vessel skeleton density (VSD), with relative differences defined on the accompanying

color scale demonstrating decreased VSD in the treated eyes. Pseudocolor flow impairment maps (column 4) demonstrate absent flow signal (white areas). The flow impairment region was markedly increased in the treated eye.

One Year Follow-Up

At 12 months after EPB, visual acuity was 0.29±0.075 (~20/40) and 0.06±0.016 (~20/20) in the treated and fellow eyes respectively (p = 0.005). 25% (4 of 16) of treated eyes with exams at this time point demonstrated at least minimal evidence of radiation retinopathy on clinical examination. Treated eyes also showed a significant lower VSD and higher FIR compared to fellow eyes (Table 2).

Two Year Follow-Up

At 24 months after EPB, visual acuity was 0.37±0.09 (~20/45) and 0.10±0.06 (~20/25) in the treated and fellow eyes respectively (p = 0.015). 75% (12 of 16) of treated eyes with exams at this time point demonstrated at least minimal evidence of radiation retinopathy on clinical examination. Treated eyes also showed a significantly lower VSD compared to fellow eyes (Table 2). In general, the difference in all metrics between treated and fellow eyes grew over time and corresponded with increasing rates of clinically identifiable radiation retinopathy in treated eyes (Figure 2).

Fig 2. Longitudinal clinical and quantitative OCTA data.

All panels reflect data from our overall cohort. Over the course of our 2-year follow-up period, there was an increasing percentage of treated eyes with clinically identifiable radiation retinopathy at each interval (A). Compared to fellow eyes over this period, treated eyes showed

decreasing vessel skeleton density (VSD) (B), increasing flow impairment region (C), and increasing vessel diameter index (D). Relative significance between treated and fellow eyes at each time point is marked by asterisks, and error bars reflect standard error of the mean.

Radiation Dose Correlation with OCTA Changes

We found significant differences in the OCTA metrics VSD and FIR over the follow-up period when the overall cohort was divided into high and low dose foveal radiation subgroups (>45 Gy [n=9] vs <15 Gy [n=3]): VSD (0.145±0.002 [high dose] (26) vs 0.154±0.001 (27), $p < 0.0001$) and FIR (2.04±0.10 (26) vs 1.59±0.06 (27), $p < 0.0001$). The VDI metric was however not significantly different between the high dose and low dose classification (2.88±0.02 (26) vs 2.83±0.08 (27), $p = 0.21$).

The five 3x3mm OCT angiograms selected for the "within eye" dose-effect analysis had the following range of radiation doses across the fovea: Case 1 - 85-250 Gy; Case 2 - 30-70 Gy; Case 3 - 25-60 Gy; Case 4 - 40-60 Gy; and Case 5 - 8-12 Gy. Of these, the case with the greatest radiation gradient across the fovea (Case 1) had EPB dosimetry gradient that spatially correlated with the microvascular gradient on the 3x3mm OCT angiogram. The longitudinal OCTA findings of Case 1 are illustrated in Figure 3, and the registered EPB dosimetry map and OCTA microvasculature is illustrated in Figure 4. The dose-dependent nature of impaired perfusion over time can be appreciated from Figure 3 when the EPB dosimetry map in Figure 4 is taken into account. The remaining cases did not appear to have any spatially correlated microvascular changes within the 3x3mm window.

Fig 3. Longitudinal skeleton density and flow impairment maps of a treated eye.

This patient is a 65-year-old male who received 212 Gy to the fovea (OD), with a range of 85-250 Gy across the standard 3x3mm OCT angiogram (Case 1). OCT angiograms were acquired at post-operative months (POM) 14, 26, and 30. The visual acuity of the treated eye at these dates was 20/25, 20/25, and 20/80 respectively. The visual acuity of the fellow eye at the same time points (OCTA images not shown) was 20/25, 20/20, and 20/25, respectively. In the skeletonized image, impaired perfusion is visible inferiorly at POM 26 compared to POM 14, with worsening perfusion at POM 30 (column 1). The loss of skeleton density is more clearly visualized in the heat map (column 2). Warmer colors reflect areas of greater vessel skeleton density, with relative differences defined on the color scale. A parallel trend is seen in the flow impairment region images (column 3).

Fig 4. Spatial correlation of parafoveal microvascular changes with radiation dose.

Panel A shows the pre-treatment fundus image of a subject (Case 1) showing the choroidal melanoma. Panel B is a computed dosimetry simulation projected onto the pre-treatment fundus image. A 3x3mm OCT angiogram of the eye was registered with the image using vessel bifurcation landmarks. Dosimetry contour lines and dosimetry tints delineate areas of the eye that received specific doses of radiation from the plaque. Panel C is an enlarged skeletonized 3x3mm OCT angiogram of the eye at post-op month 30 with the corresponding dosimetry contour lines. Note the inferior areas of decreased vascular density (impaired perfusion) in the 3x3mm image, which corresponds with the higher doses delivered inferiorly.

Discussion

This study adds to a body of literature that has demonstrated retinal microvascular changes after episcleral plaque brachytherapy (EPB). Specifically, our study demonstrated a significant decrease in capillary density in EPB treated eyes earlier than previously reported and prior to clinically evident radiation retinopathy. It also demonstrated progressive decreases in density at intervals over a 2-year period. This was accomplished through the use of quantitative metrics that directly reflect microvascular density such as vessel skeleton density (VSD), and also indirectly such as flow impairment region (FIR). Significant changes in vessel diameter index (VDI) were also seen over this time period. In addition to these findings, we present a case with a large gradient (>165 Gy) of high-dose radiation across the fovea that appears to be spatially correlated to microvascular density. Collectively, these data suggest that capillary changes are occurring before clinically evident retinopathy, and that the magnitude of the radiation dose may correlate with the magnitude of the capillary damage in any given region. Furthermore, they highlight the potential utility of OCTA to monitor the progression of subtle changes in microvasculature over a period of months in treated eyes.

Our findings were consistent with those in prior studies that used OCTA to assess parafoveal vessel density in irradiated eyes. Say et al. and Cennamo et al quantified total vascular area using 3x3mm and 6x6mm binarized en-face images, respectively.(14, 15) Both demonstrated significant reduction in vessel area density in irradiated eyes compared to fellow eyes. Although the capillary densities in these previous studies were estimated as vessel area density, our preferred method for estimating capillary density is the skeletonized density (VSD). This is because VSD is not influenced by capillary morphologic changes such as vessel diameter, which

283 may accompany vasculopathies, and is also minimally impacted by large caliber vessels. For
284 brevity, our study only reports the VSD analysis as the measure for capillary density. Vessel
285 diameter was approximated as an index -VDI - which we also demonstrate changes with
286 worsening retinopathy . FIR, our third metric, complements VSD as an indirect measure of
287 density and a direct measure of subclinical impaired perfusion. As FIR only accounts for
288 avascular areas above a set threshold, it theoretically has a higher specificity (but lower
289 sensitivity) for capillary dropout. For example, the loss of very minute areas of capillary flow
290 may not result in an avascular area above our set threshold, and therefore would have no effect
291 on FIR, but a definite effect on VSD.
292
293 The findings of our study highlight the potential use of OCTA for monitoring vascular changes
294 in irradiated eyes over time. The vascular metrics can also serve as adjuncts to help grade the
295 severity of radiation retinopathy. Several groups have aimed to develop effective grading
296 schemes that use various imaging modalities, including ultra-wide field fluorescein
297 angiography.(9) In 2005, Finger et al developed a system with four stages of severity that
298 correlated with vision loss, based on a combination of findings from dye-based angiography and
299 ophthalmoscopy.(8) Horgan et al later described in 2008 how OCT could be further added to
300 identify macular edema, an early clinical feature of radiation retinopathy.(7) More recently,
301 Veverka et al. suggested OCTA could also be used to help grade severity, demonstrating that it
302 may detect RR prior to changes seen on OCT alone.(28)
303
304 Thus, we concur with the assertion that OCTA may be a powerful tool in determining the
305 severity of radiation retinopathy, and also in detecting very early microvascular changes before

the onset of retinopathy on exam. This has a wide variety of clinical applications. For example, OCTA can contribute relevant information for individualizing the time point for RR treatment intervention, and also provide sensitive biomarkers for comparing the efficacy of RR treatment regimens.(29-31) The use of various metrics as demonstrated in this study may noticeably increase the sensitivity of OCTA to capture early changes in RR, as subtle changes in density and vessel diameter are often challenging to appreciate qualitatively in the clinic setting. For clinical purposes, we suggest obtaining 3x3mm OCT angiograms in both eyes prior to EPB placement, and intermittently at follow-up visits for those with access to these devices. As our study has shown, significant microvascular changes can be seen within 6 months of treatment, suggesting repeat imaging may be prudent at early post-operative dates. Furthermore, as our understanding of the utility of OCTA continues to grow, longitudinal scans may prove useful in the long-term management of individuals with RR including indications for therapy.

Our exploration of a possible spatial correlation between radiation dose and capillary density was demonstrated in Case 1 (Figure 4) which had (by chance alone) a very steep gradient change for the radiation dose over the 3x3mm area of the macula which was imaged. Of note, Case 4 also showed a large area of ischemia nearest the high dose radiation in a wider 6x6mm window. The significantly lower resolution of 6x6mm OCTA scans precludes a detailed analysis of density changes in these scans. Our findings provide a basis for future studies assessing the within eye spatial relation between EPB dosimetry and microvasculature abnormalities to enhance the understanding of radiation dose on the retinal vasculature and the development of radiation retinopathy.

Some potential limitations of our study include those inherent to OCTA imaging, such as motion artifacts and floaters, which can interfere with efforts to accurately quantify vascular metrics. We aimed to control for this by excluding images with significant artifacts. Additionally, this study analyzed images from the 3x3mm OCTA scan pattern and may have missed some peripheral defects associated with EPB. However, larger scan patterns available at the time of this study did not have sufficient resolution to reliably detect capillary level changes, so use of the high resolution 3x3mm field was necessary. Future studies may consider images from 6x6mm or even larger windows if the resolution of the scans is sufficient. Furthermore, future studies may aim to generate dosimetry maps in a larger number of eyes, and employ more quantitative approaches to better evaluate the spatial relationship between EPB dosimetry and microvascular aberrations. Other limitations are from the retrospective nature of the data analyzed. For example, the images for the study were acquired during study visits which were determined on a case to case basis by the physician. Although we addressed the difference in the time intervals by binning, our findings can be refined by using a regularized and standardized time intervals across subjects.

In conclusion, we investigated OCTA changes associated with EPB treatment of choroidal melanoma and report significant changes in OCTA metrics at about 6 months or earlier, even when there were no clinically detectable signs of radiation retinopathy. The change in the OCTA metrics increased over time, and in a dose dependent manner. We infer that OCTA can be a viable tool for monitoring the effect of EPB on the retinal microvasculature and its findings may play a pivotal role in developing intervention modalities to delay or treat the occurrences of retinopathy after episcleral plaque brachytherapy.

References

1. Group COMS. The COMS randomized trial of iodine 125 brachytherapy for choroidal melanoma: V. Twelve-year mortality rates and prognostic factors: COMS report No. 28. Arch Ophthalmol. 2006;124(12):1684-93.
2. Melia BM, Abramson DH, Albert DM, Boldt HC, Earle JD, Hanson WF, et al. Collaborative ocular melanoma study (COMS) randomized trial of I-125 brachytherapy for medium choroidal melanoma. I. Visual acuity after 3 years COMS report no. 16. Ophthalmology. 2001;108(2):348-66.
3. Berry JL, Dandapani SV, Stevanovic M, Lee TC, Astrahan M, Murphree AL, et al. Outcomes of choroidal melanomas treated with eye physics: a 20-year review. JAMA Ophthalmol. 2013;131(11):1435-42.
4. Le BHA, Kim JW, Deng H, Rayess N, Jennelle RL, Zhou SY, et al. Outcomes of choroidal melanomas treated with eye physics plaques: A 25-year review. Brachytherapy. 2018;17(6):981-9.
5. Durkin SR, Roos D, Higgs B, Casson RJ, Selva D. Ophthalmic and adnexal complications of radiotherapy. Acta Ophthalmol Scand. 2007;85(3):240-50.
6. Archer DB, Amoaku WM, Gardiner TA. Radiation retinopathy--clinical, histopathological, ultrastructural and experimental correlations. Eye (Lond). 1991;5 (Pt 2):239-51.
7. Horgan N, Shields CL, Mashayekhi A, Teixeira LF, Materin MA, Shields JA. Early macular morphological changes following plaque radiotherapy for uveal melanoma. Retina. 2008;28(2):263-73.
8. Finger PT, Kurli M. Laser photocoagulation for radiation retinopathy after ophthalmic plaque radiation therapy. Br J Ophthalmol. 2005;89(6):730-8.
9. McCannel TA, Kim E, Kamrava M, Lamb J, Caprioli J, Yang D, et al. NEW ULTRA-WIDE-FIELD ANGIOGRAPHIC GRADING SCHEME FOR RADIATION RETINOPATHY AFTER IODINE-125 BRACHYTHERAPY FOR UVEAL MELANOMA. Retina. 2018;38(12):2415-21.
10. Kashani AH, Chen CL, Gahm JK, Zheng F, Richter GM, Rosenfeld PJ, et al. Optical coherence tomography angiography: A comprehensive review of current methods and clinical applications. Prog Retin Eye Res. 2017;60:66-100.
11. Kim AY, Chu Z, Shahidzadeh A, Wang RK, Puliafito CA, Kashani AH. Quantifying Microvascular Density and Morphology in Diabetic Retinopathy Using Spectral-Domain Optical Coherence Tomography Angiography. Investigative ophthalmology & visual science. 2016;57(9):Oct362-70.
12. Koulisis N, Kim AY, Chu Z, Shahidzadeh A, Burkemper B, Olmos de Koo LC, et al. Quantitative Microvascular Analysis of Retinal Venous Occlusions by Spectral Domain Optical Coherence Tomography Angiography. Association for Research in Vision and Ophthalmology (ARVO) Abstract 5505 - C0109; Seattle, WA2016.
13. Kim AY, Rodger DC, Shahidzadeh A, Chu Z, Koulisis N, Burkemper B, et al. Quantifying Retinal Microvascular Changes in Uveitis Using Spectral-Domain Optical Coherence Tomography Angiography. American journal of ophthalmology. 2016;171:101-12.
14. Cennamo G, Breve MA, Velotti N, Sparnelli F, Iovino C, Farella A, et al. Evaluation of Vascular Changes with Optical Coherence Tomography Angiography after Plaque Radiotherapy of Choroidal Melanoma. Ophthalmic Res. 2018:1-5.

15. Say EA, Samara WA, Khoo CT, Magrath GN, Sharma P, Ferenczy S, et al. PARAFOVEAL CAPILLARY DENSITY AFTER PLAQUE RADIOTHERAPY FOR CHOROIDAL MELANOMA: Analysis of Eyes Without Radiation Maculopathy. Retina. 2016;36(9):1670-8.
16. Parrozzani R, Frizziero L, Londei D, Trainiti S, Modugno RL, Leonardi F, et al. Peripapillary vascular changes in radiation optic neuropathy: an optical coherence tomography angiography grading. Br J Ophthalmol. 2018;102(9):1238-43.
17. Skalet AH, Liu L, Binder C, Miller AK, Wang J, Wilson DJ, et al. Quantitative OCT Angiography Evaluation of Peripapillary Retinal Circulation after Plaque Brachytherapy. Ophthalmol Retina. 2018;2(3):244-50.
18. Chu Z, Lin J, Gao C, Xin C, Zhang Q, Chen CL, et al. Quantitative assessment of the retinal microvasculature using optical coherence tomography angiography. J Biomed Opt. 2016;21(6):66008.
19. Berry JL, Kim JW, Jennelle R, Astrahan M. Use of the Toric Surgical Marker to Aid in Intraoperative Plaque Placement for the USC Eye Physics Plaques to Treat Uveal Melanoma: A New Surgical Technique. Ophthalmic Surg Lasers Imaging Retina. 2015;46(8):866-70.
20. Michaelson, IC. Retinal circulation in man and animals. Springfield, Illinois: Charles C: Thomas Publisher; 1954.
21. Ying GS, Maguire MG, Glynn R, Rosner B. Tutorial on Biostatistics: Statistical Analysis for Correlated Binary Eye Data. Ophthalmic Epidemiol. 2018;25(1):1-12.
22. Grimm J, LaCouture T, Croce R, Yeo I, Zhu Y, Xue J. Dose tolerance limits and dose volume histogram evaluation for stereotactic body radiotherapy. J Appl Clin Med Phys. 2011;12(2):3368.
23. Astrahan MA, Luxton G, Jozsef G, Kampp TD, Liggett PE, Sapozink MD, et al. An interactive treatment planning system for ophthalmic plaque radiotherapy. Int J Radiat Oncol Biol Phys. 1990;18(3):679-87.
24. Astrahan MA, Luxton G, Pu Q, Petrovich Z. Conformal episcleral plaque therapy. Int J Radiat Oncol Biol Phys. 1997;39(2):505-19.
25. Astrahan MA. Improved treatment planning for COMS eye plaques. Int J Radiat Oncol Biol Phys. 2005;61(4):1227-42.
26. Group A-REDSR. A randomized, placebo-controlled, clinical trial of high-dose supplementation with vitamins C and E, beta carotene, and zinc for age-related macular degeneration and vision loss: AREDS report no. 8. Arch Ophthalmol. 2001;119(10):1417-36.
27. Birch DG, Bennett LD, Duncan JL, Weleber RG, Pennesi ME. Long-term Follow-up of Patients With Retinitis Pigmentosa Receiving Intraocular Ciliary Neurotrophic Factor Implants. Am J Ophthalmol. 2016;170:10-4.
28. Veverka KK, AbouChehade JE, Iezzi R, Pulido JS. NONINVASIVE GRADING OF RADIATION RETINOPATHY: The Use of Optical Coherence Tomography Angiography. Retina. 2015;35(11):2400-10.
29. Murray TG, Latiff A, Villegas VM, Gold AS. Aflibercept for Radiation Maculopathy Study: A Prospective, Randomized Clinical Study. Ophthalmology Retina. 2019;3(7):561-6.
30. Stacey AW, Demirci H. Serial Intravitreal Bevacizumab Injections Slow the Progression of Radiation Maculopathy Following Iodine-125 Plaque Radiotherapy. The open ophthalmology journal. 2016;10:103-10.
31. Houston SK, Shah NV, Decatur C, Lonngi M, Feuer W, Markoe AM, et al. Intravitreal bevacizumab combined with plaque brachytherapy reduces melanoma tumor volume and

441 enhances resolution of exudative detachment. Clinical ophthalmology (Auckland, NZ).
442 2013;7:193-8.
443

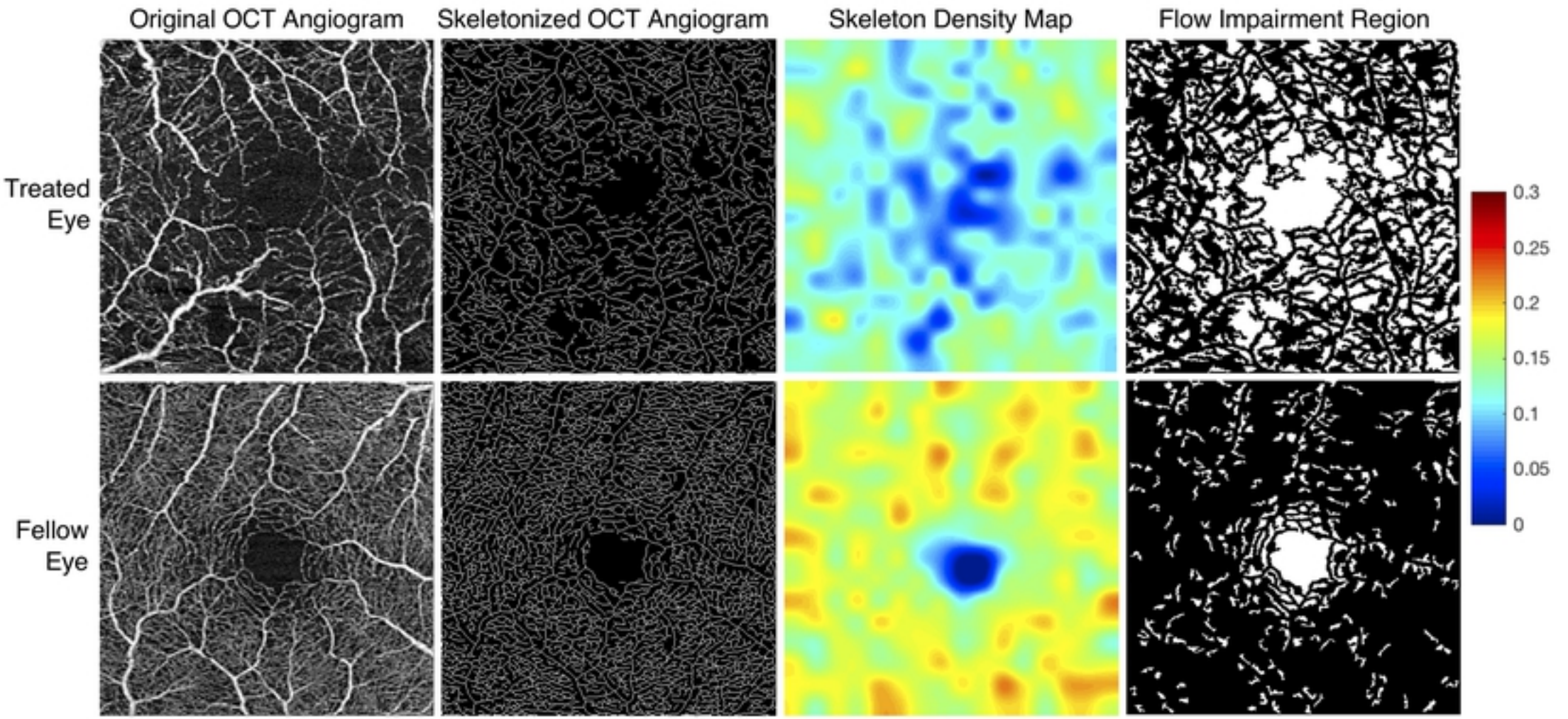

Figure 1. Processed OCT angiograms from treated and fellow eyes of a single patient.

Figure 1

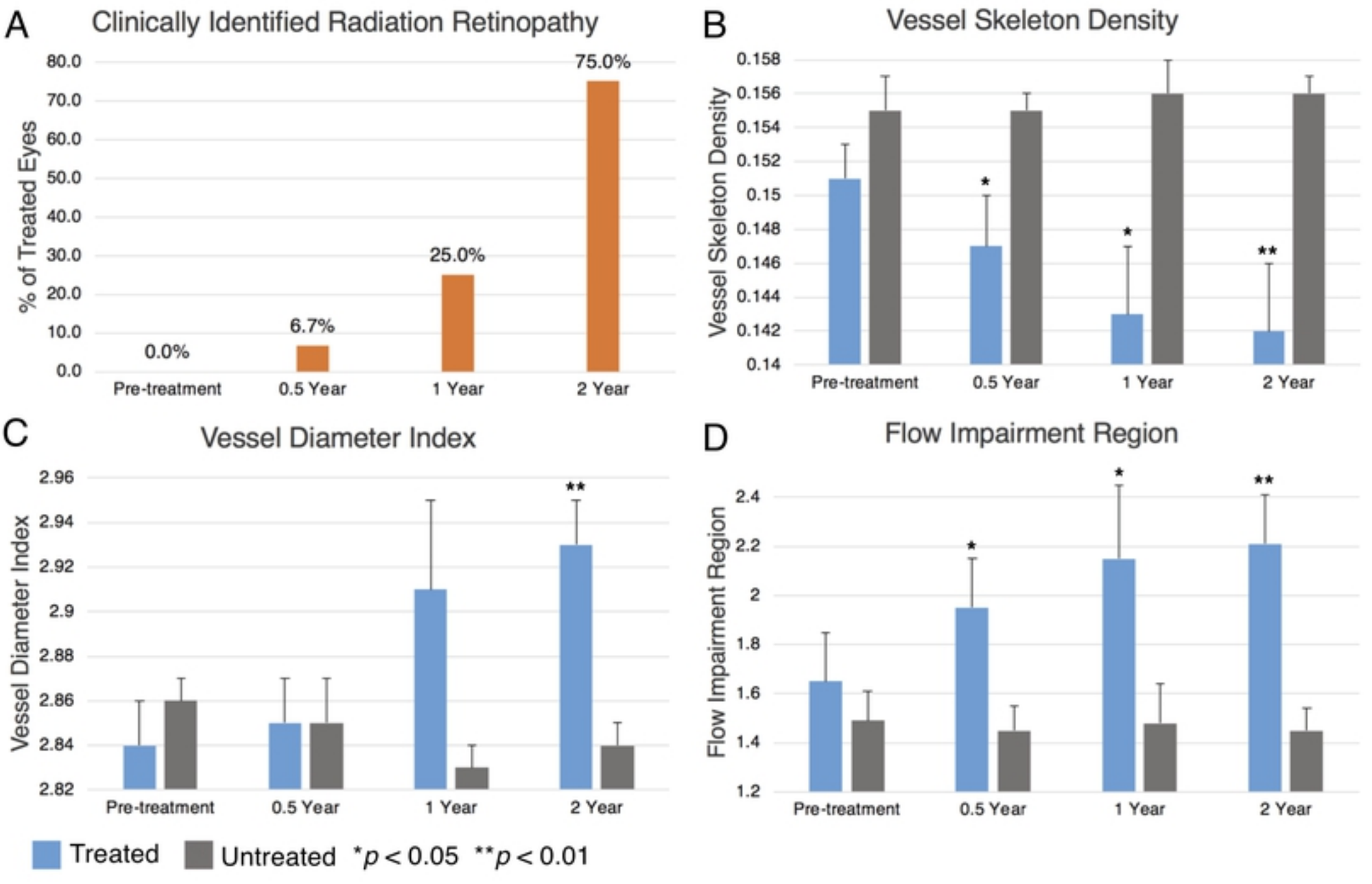

Figure 2. Longitudinal clinical and quantitative OCTA data.

Figure 2

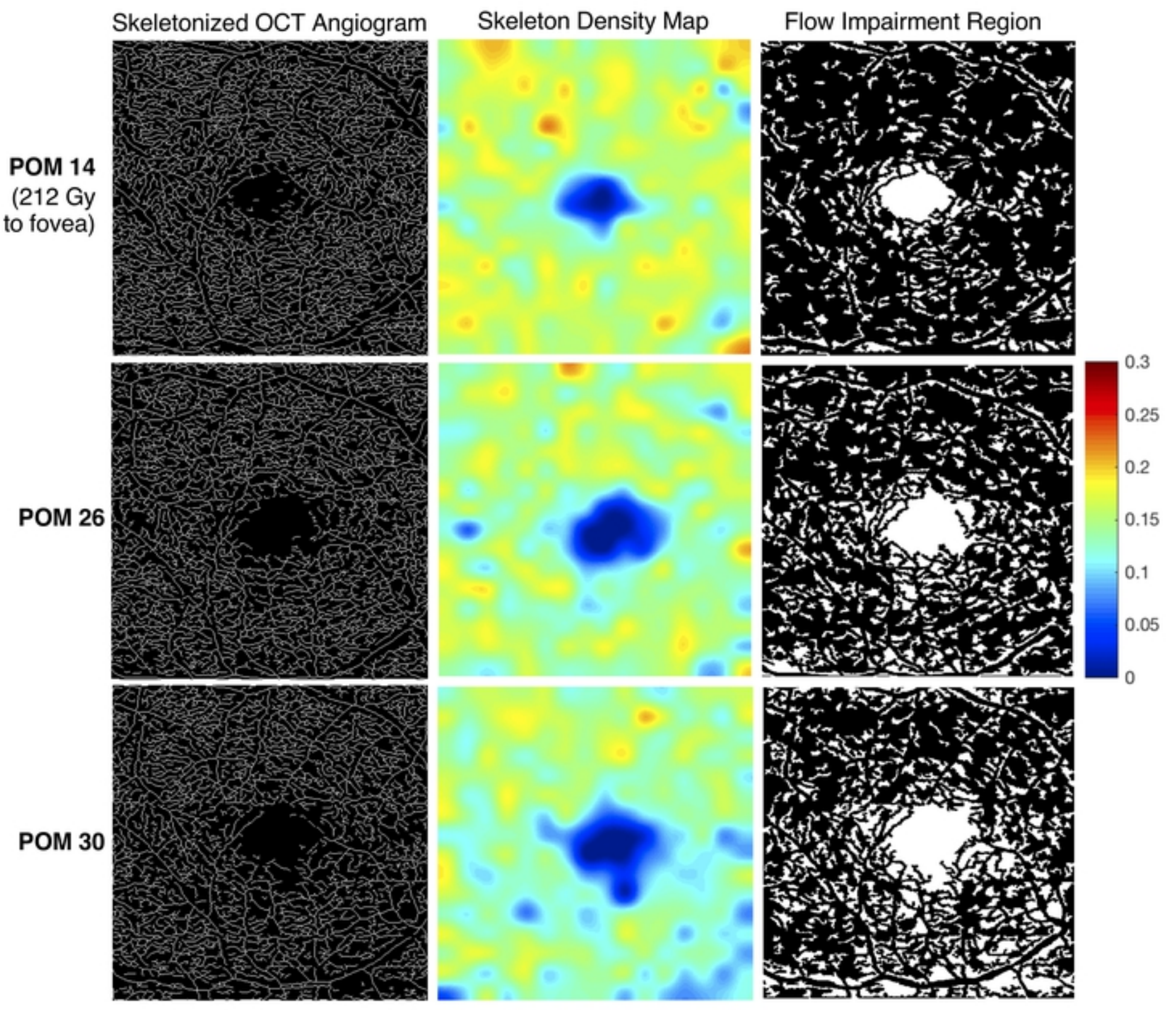

Figure 3. Longitudinal skeleton density and flow impairment maps of a treated eye.

Figure 3

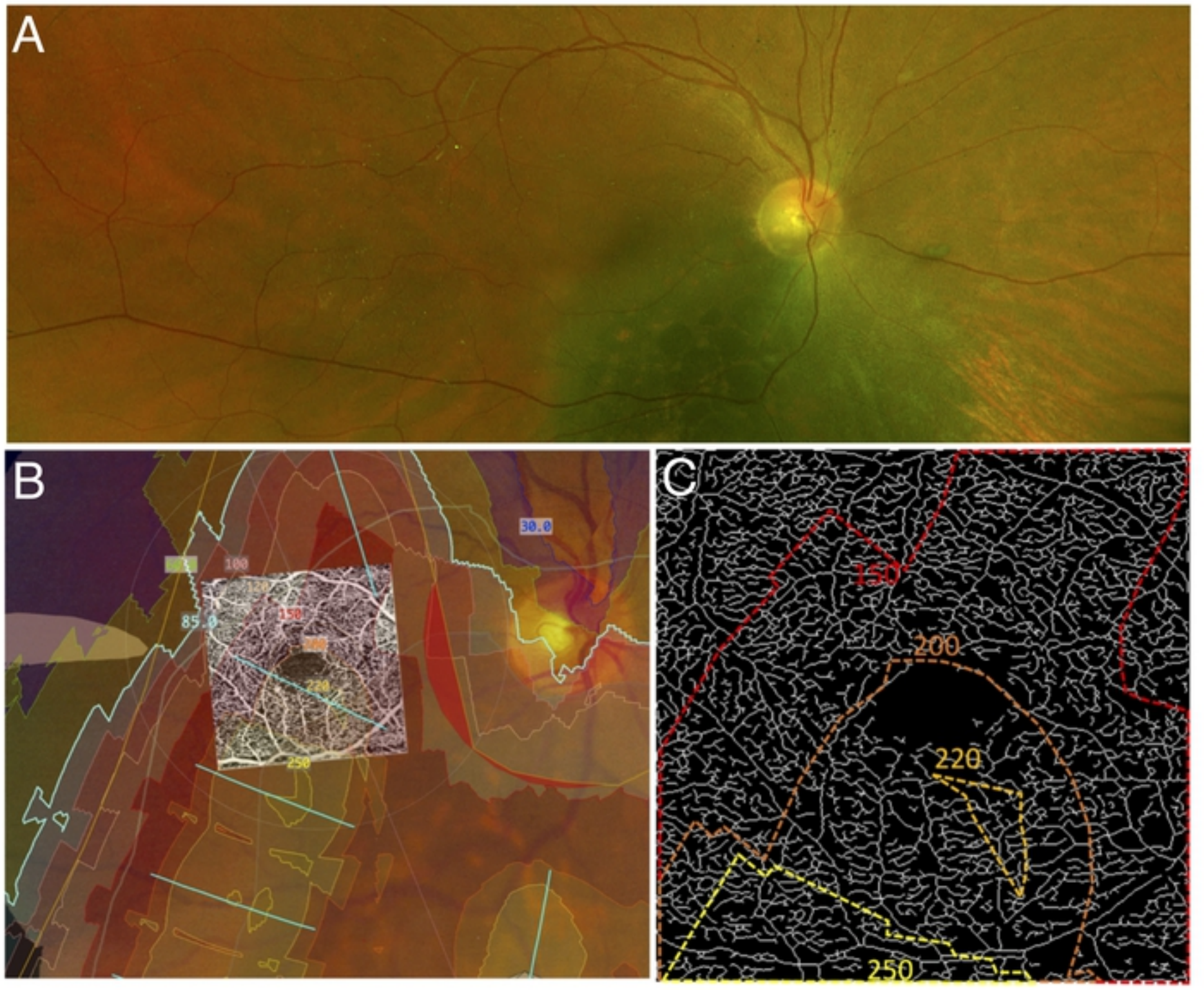

Figure 4. Spatial correlation of parafoveal microvascular changes with radiation dose.

Figure 4